

# Thermal convection for large Prandtl numbers

Siegfried Grossmann<sup>1</sup> and Detlef Lohse<sup>2</sup>

<sup>1</sup> *Department of Physics, University of Marburg, Renthof 6, D-35032 Marburg, Germany*

<sup>2</sup> *Department of Applied Physics and J. M. Burgers Centre for Fluid Dynamics, University of Twente, 7500 AE Enschede, Netherlands*

(February 8, 2008)

The Rayleigh-Benard theory by Grossmann and Lohse [J. Fluid Mech. 407, 27 (2000)] is extended towards very large Prandtl numbers  $Pr$ . The Nusselt number  $Nu$  is found here to be independent of  $Pr$ . However, for fixed Rayleigh numbers  $Ra > 10^{10}$  a maximum around  $Pr \approx 2$  in the  $Nu(Pr)$ -dependence is predicted which is absent for lower  $Ra$ . We moreover offer the full functional dependences of  $Nu(Ra, Pr)$  and  $Re(Ra, Pr)$  within this extended theory, rather than only giving the limiting power laws as done in ref. [1]. This enables us to more realistically describe the *transitions* between the various scaling regimes, including their widths.

In thermal convection, the control parameters are the Rayleigh number  $Ra$  and the Prandtl number  $Pr$ . The system responds with the Nusselt number  $Nu$  (the dimensionless heat flux) and the Reynolds number  $Re$  (the dimensionless large scale velocity). The key question is to understand the dependences  $Nu(Ra, Pr)$  and  $Re(Ra, Pr)$ . In experiments, traditionally the Prandtl number was more or less kept fixed [2–4]. However, the recent experiments in the vicinity of the critical point of helium gas [5, 6] and of  $SF_6$  [7] or with various alcohols [8] allow to vary both  $Ra$  and  $Pr$  and thus to explore a larger domain of the  $Ra-Pr$  parameter space of Rayleigh-Benard (RB) convection, in particular that for  $Pr \gg 1$ . While the experiments of Steinberg's group [7] suggest a decreasing Nusselt number with increasing  $Pr$ , namely  $Nu = 0.22Ra^{0.3 \pm 0.03}Pr^{-0.2 \pm 0.04}$  in  $10^9 \leq Ra \leq 10^{14}$  and  $1 \leq Pr \leq 93$ , the experiments of the Ahlers group suggest a saturation of  $Nu$  with increasing  $Pr$  for fixed  $Ra$ , at least up to  $Ra = 10^{10}$  [9]. The same saturation (at fixed  $Ra = 6 \cdot 10^5$ ) is found in the numerical simulations by Verzicco and Camussi [10] and Herring and Kerr [11].

The large  $Pr$  regime of the latest experiments has not been covered by the recent theory on thermal convection by Grossmann and Lohse (GL, [1]), which otherwise does pretty well in accounting for various measurements. In particular, it explains the low  $Pr$  measurements of Cioni et al. [4] ( $Pr = 0.025$ ), the low  $Pr$  numerics which reveal  $Nu \sim Pr^{0.14}$  for fixed  $Ra$  [10, 11], and the above mentioned experiments by Niemela et al. [6] and Xu et al. [8].

In the present paper we extend the GL theory in a natural way to the regime of very large  $Pr$ , on which no statement has been made in the original paper [1]. We find  $Nu$  to be independent of  $Pr$  in that regime. We in addition present the complete functional dependences  $Nu(Ra, Pr)$  and  $Re(Ra, Pr)$  within the GL theory, rather than only giving the limiting power laws and superpositions of those as was done in [1]. This enables us to more realistically describe the *transitions* between the various scaling regimes found already in [1].

*Approach:* To make this paper selfcontained we very briefly recapitulate the key idea of the GL theory, which is to decompose in the volume averages of the energy dissipation rate  $\epsilon_u$  and the thermal dissipation rate  $\epsilon_\theta$  into their boundary layer (BL) and bulk contributions,

$$\epsilon_u = \epsilon_{u,BL} + \epsilon_{u,bulk}, \quad (1)$$

$$\epsilon_\theta = \epsilon_{\theta,BL} + \epsilon_{\theta,bulk}. \quad (2)$$

For the left hand sides the exact relations  $\epsilon_u = \frac{\nu^3}{L^4}(Nu - 1)RaPr^{-2}$  and  $\epsilon_\theta = \kappa \frac{\Delta^2}{L^2}Nu$  are used, where  $\nu$  is the kinematic viscosity,  $\kappa$  the thermal diffusivity,  $L$  the height of the cell, and  $\Delta$  the temperature difference between the bottom and the top plates. Next, the local dissipation rates in the BL and in the bulk (right hand sides of eqs. (1) and (2)) are modelled as the corresponding energy input rates, i.e., in terms of  $U$ ,  $\Delta$ , and the widths  $\lambda_u$  and  $\lambda_\theta$  of the kinetic and thermal boundary layers, respectively. For the thickness of the thermal BL we assume  $\lambda_\theta = L/(2Nu)$  and for that of the kinetic one  $\lambda_u = L/(4\sqrt{Re})$  as it holds in Blasius type layers [12]; as for the prefactor 1/4 cf. [1], Sec. 4.3. For very large  $Ra$  the laminar BL will become turbulent and  $\lambda_u$  will show a stronger  $Re$  dependence. Note that whereas the thermal BLs only build up at the top and bottom wall, the kinetic BL occurs at *all* walls of the cell and therefore the contribution of  $\epsilon_{u,BL}$  to  $\epsilon_u$  is larger than a simple minded argument would suggest. The two eqs. (1) and (2) then allow to calculate the two dependent variables  $Nu$  and  $Re$  as functions of the two independent ones  $Ra$  and  $Pr$ .

*Input rate modeling:* The modeling of the dissipation rates on the rhs of eqs. (1) and (2) is guided by the Boussinesq equations. Depending on whether the BL or the bulk contributions are dominant, one gets different expressions on the rhs of eqs. (1), (2) and thus different relations for  $Nu$ ,  $Re$  vs.  $Ra$ ,  $Pr$ , defining different main regimes, see ref. [1] and fig. 1.

The rhs thermal dissipation rates depend on whether the kinetic BL of thickness  $\lambda_u$  is within the thermal BL of thickness  $\lambda_\theta$  ( $\lambda_u < \lambda_\theta$ , small  $Pr$ ) or vice versa ( $\lambda_u > \lambda_\theta$ , large  $Pr$ ). The line  $\lambda_u = \lambda_\theta$ , corresponding to  $Nu = 2\sqrt{Re}$ , splits the phase diagram into a lower (small  $Pr$ ) and an upper (large  $Pr$ ) part, which we shall label by “ $\ell$ ” and “ $u$ ”.

We first consider  $\lambda_u < \lambda_\theta$  (i.e., small  $Pr$ , regime “ $\ell$ ”). Then (see [1])

$$\epsilon_{u,bulk} \sim \frac{U^3}{L} \sim \frac{\nu^3}{L^4}Re^3, \quad (3)$$

$$\epsilon_{u,BL} \sim \nu \frac{U^2 \lambda_u}{\lambda_u^2 L} \sim \frac{\nu^3}{L^4}Re^{5/2}, \quad (4)$$

$$\epsilon_{\theta,bulk} \sim \frac{U\Delta^2}{L} \sim \kappa \frac{\Delta^2}{L^2}PrRe, \quad (5)$$

$$\epsilon_{\theta,BL} \sim \kappa \frac{\Delta^2}{L^2}(RePr)^{1/2}. \quad (6)$$

The last expression is concluded [1, 3, 13] from the heat transfer equation  $u_x \partial_x \theta + u_z \partial_z \theta = \kappa \partial_z^2 \theta$ , which implies  $U/L \sim \kappa/\lambda_\theta^2$  giving  $Re^{1/2}Pr^{1/2} \sim Nu$ .

If now larger  $Pr$  are considered, the kinetic boundary will eventually exceed the thermal one,  $\lambda_u > \lambda_\theta$ , upper range “ $u$ ”. The relevant velocity at the edge between the thermal BL and the thermal bulk now is less than  $U$ , about  $U\lambda_\theta/\lambda_u$ . To describe the transition from  $\lambda_u$  being smaller to being larger than  $\lambda_\theta$  we introduce the function  $f(x) = (1 + x^n)^{-1/n}$  of the variable  $x_\theta = \lambda_u/\lambda_\theta = c_\theta Nu/2\sqrt{Re}$ ,  $f$  being 1 in the lower range “ $\ell$ ” (small  $Pr$ ) and  $1/x_\theta$

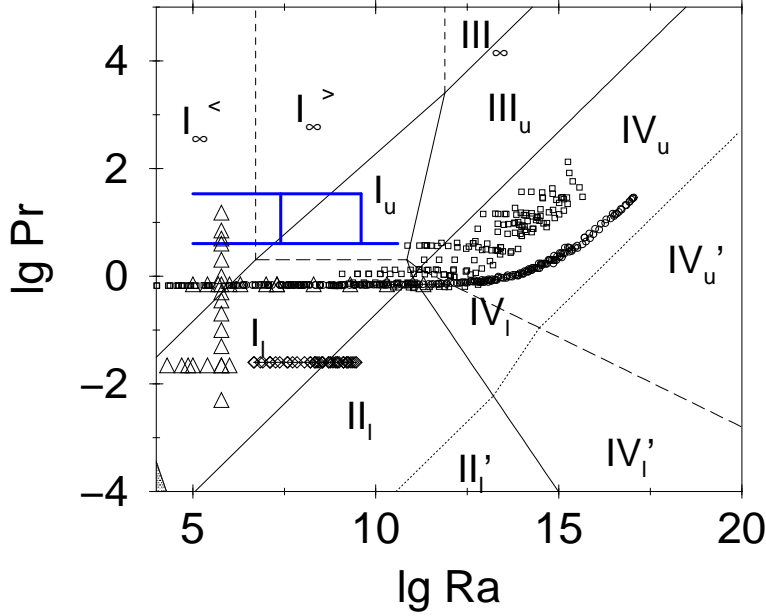


FIG. 1. Phase diagram in the  $Ra - Pr$  plane, with data points included where  $Nu$  has been measured or numerically calculated. Squares show measuring points of Chavanne et al. [5], diamonds those by Cioni et al. [4], circles those by Niemela et al. [6], the very thick lines those by Xu et al. [8], and the triangles are those points for which Verzicco and Camussi did full numerical simulations [10]. The long-dashed line is the line  $\lambda_u = \lambda_\theta$ . The thin dotted line denotes where the laminar kinetic BL becomes turbulent. As extensively discussed in ref. [1], the exact onset of this instability strongly depends on the prefactors used when calculating this type of phase diagram. For this phase diagram the same prefactors as in ref. [1] have been chosen.

in “ $u$ ” (large  $Pr$ ), respectively.  $c_\theta$  is about 1. The relevant velocity then is  $Uf(x_\theta)$ . We take  $n = 4$  to characterize the sharpness of the transition.

This generalizes (5), (6) to

$$\epsilon_{\theta,bulk} \sim \kappa \frac{\Delta^2}{L^2} Pr Re f(c_\theta Nu / 2\sqrt{Re}), \quad (7)$$

$$\epsilon_{\theta,BL} \sim \kappa \frac{\Delta^2}{L^2} \sqrt{Pr Re f(c_\theta Nu / 2\sqrt{Re})}, \quad (8)$$

while  $\epsilon_{u,bulk}$  and  $\epsilon_{u,BL}$  are still given by (3),(4). Introducing (7),(8),(3),(4) into (1),(2) leads to the  $Ra, Pr$  dependences of  $Nu, Re$  in the upper regime “ $u$ ”. The pure power laws  $Nu(Ra, Pr)$  and  $Re(Ra, Pr)$  in both the *lower* “ $\ell$ ” ( $\lambda_u < \lambda_\theta$ , small  $Pr$ ) and the *upper* “ $u$ ” ( $\lambda_u > \lambda_\theta$ , large  $Pr$ ) regimes are summarized in table I.

*Very large  $Pr$  regime:* We now extend the theory to very large Prandtl numbers. As long as  $Ra > Ra_c = 1708$  there still is wind, even for very large  $Pr$ , as  $Ra_c$  is independent of  $Pr$ . However, to keep  $Ra$  fixed, one has to increase the temperature difference  $\Delta$  with

regime	dominance of	BLs	$Nu$	$Re$
$I_l$	$\epsilon_{u,BL}, \epsilon_{\theta,BL}$	$\lambda_u < \lambda_\theta$	$Ra^{1/4} Pr^{1/8}$	$Ra^{1/2} Pr^{-3/4}$
$I_u$		$\lambda_u > \lambda_\theta$	$Ra^{1/4} Pr^{-1/12}$	$Ra^{1/2} Pr^{-5/6}$
$I_\infty^<$		$\lambda_u = L/4 > \lambda_\theta$	$Ra^{1/3}$	$Ra^{2/3} Pr^{-1}$
$I_\infty^>$		$\lambda_u = L/4 > \lambda_\theta$	$Ra^{1/5}$	$Ra^{3/5} Pr^{-1}$
$II_l$	$\epsilon_{u,bulk}, \epsilon_{\theta,BL}$	$\lambda_u < \lambda_\theta$	$Ra^{1/5} Pr^{1/5}$	$Ra^{2/5} Pr^{-3/5}$
$III_u$	$\epsilon_{u,BL}, \epsilon_{\theta,bulk}$	$\lambda_u > \lambda_\theta$	$Ra^{3/7} Pr^{-1/7}$	$Ra^{4/7} Pr^{-6/7}$
$III_\infty$		$\lambda_u = L/4 > \lambda_\theta$	$Ra^{1/3}$	$Ra^{2/3} Pr^{-1}$
$IV_l$	$\epsilon_{u,bulk}, \epsilon_{\theta,bulk}$	$\lambda_u < \lambda_\theta$	$Ra^{1/2} Pr^{1/2}$	$Ra^{1/2} Pr^{-1/2}$
$IV_u$		$\lambda_u > \lambda_\theta$	$Ra^{1/3}$	$Ra^{4/9} Pr^{-2/3}$

TABLE I. The power laws for  $Nu$  and  $Re$  of the presented theory. The regimes  $II_u$  and  $III_l$  are not included as they do not or hardly exist for the choice of prefactors.

increasing  $\nu$  or  $Pr$ .  $Pr \gg 1$  will lead to a smaller and smaller large scale wind  $Re$ . The flow will eventually become laminar throughout the cell.  $\lambda_u$  can no longer continue to increase according to  $\lambda_u \sim Re^{-1/2}$  with decreasing  $Re$ , but will saturate to a constant value of order  $L$ . This is the central new point of the very large  $Pr$  regime. In [1] we had assumed that this happens at about  $Re = 50$ . This corresponds to a saturation at  $\lambda_u = L/4\sqrt{Re} = L/28$ . To model the smooth transition to the very large  $Pr$  regime beyond the line  $Re = 50$ , i.e., if  $\lambda_u = L/4\sqrt{Re}$  approaches  $\lambda_u = L/28$  we use the crossover function  $g(x) = x(1 + x^n)^{-1/n}$  of the crossover variable  $x_L = 28\lambda_u/L = 7/\sqrt{Re}$ , and again  $n = 4$ . The function  $g$  increases linearly,  $g(x_L) = x_L$ , below the transition ( $x_L$  small) and is 1 in the very large  $Pr$  regime with  $Re \leq 50$ . In the above modelings for the local dissipation rates we have to replace each  $\lambda_u$  by  $g(x_L)L/28$ .

The resulting formulae, given momentarily, will lead, depending on  $Ra$ , to three new regimes, valid for very large  $Pr$ , denoted as  $I_\infty^<$ ,  $I_\infty^>$ , and  $III_\infty$ , see Fig. 1 and Table I.

While eq. (3) for  $\epsilon_{u,bulk}$  is assumed to still hold in the very large  $Pr$  range (where  $\epsilon_{u,bulk}$  of course hardly contributes to  $\epsilon_u$  due to the large extension of the kinetic BLs), eqs. (4), (5), and (6) have to be generalized. First generalize (4) for  $\epsilon_{u,BL}$ ,

$$\epsilon_{u,BL} \sim \nu \frac{U^2}{g(x_L)L^2} \sim \frac{\nu^3}{L^4} \frac{Re^2}{g(7/\sqrt{Re})}. \quad (9)$$

Next  $\epsilon_{\theta,bulk}$ : Above the wind velocity  $U$  in (5), which sets the time scale of the stirring, has already been generalized to  $Uf(\lambda_u/\lambda_\theta)$ . This equals  $U$  itself in “ $\ell$ ” and  $U\lambda_\theta/\lambda_u$  in the “ $u$ ” regimes. Now in addition the explicit  $\lambda_u$  is to be replaced by  $g(x_L)L/28$ , i.e.,

$$\epsilon_{\theta,bulk} \sim \kappa \frac{\Delta^2}{L^2} Pr Re \ f\left(\frac{Nu}{14} g\left(\frac{7}{\sqrt{Re}}\right)\right). \quad (10)$$

This simplifies for large enough  $Ra$  (therefore large  $f$ -argument) and very large  $Pr$  (thus large  $g$ -argument) to

$$\epsilon_{\theta,bulk} \sim \kappa \frac{\Delta^2}{L^2} \frac{Pr Re}{Nu}. \quad (11)$$

Inserting (9) and (11) into the rhs of (1) and (2) leads to the new power laws describing the heat flux and the wind velocity in the regime  $III_\infty$  beyond  $III_u$ , cf. Figure 1,

$$Nu \sim Ra^{1/3} Pr^0, \quad Re \sim Ra^{2/3} Pr^{-1}. \quad (12)$$

Finally  $\epsilon_{\theta,BL}$ : In the thermal boundary layer range beyond  $I_\ell$ , relevant for medium  $Ra$ , eq.(6) stays valid, because its derivation did not involve  $\lambda_u$  and also  $f = 1$ . The range  $I_\infty^<$  has to be described by eqs.(1),(2),(9) (with  $g = 1$ ), and (6), resulting in the same power laws as in regime  $III_\infty$ , i.e., eqs. (12). For  $Pr$  values above regime  $I_u$  eq.(6) no longer holds. It originated from the heat transport equation. There we have to use now  $Uf(x_\theta)$  instead of merely  $U$ . The balance from the heat transfer equation then reads  $Uf(x_\theta)/L \sim \kappa/\lambda_\theta^2$ . In the  $f$ -argument  $x_\theta = \lambda_u/\lambda_\theta$  the kinetic BL width  $\lambda_u$  and therefore the crossover function  $g$  appears, leading to

$$Pr Re f \left( \frac{Nu}{14} g \left( \frac{7}{\sqrt{Re}} \right) \right) \sim Nu^2. \quad (13)$$

In the very large  $Pr$  regime (where  $g(x_L) = 1$ ) above  $I_u$  (where  $f(x_\theta) = x_\theta^{-1}$ ) one obtains from (13) the relation  $(Re Pr)^{1/3} \sim Nu$ , valid in  $I_\infty^>$ . Together with (1), (2), and (9) one derives the new scaling laws in the interior of  $I_\infty^>$

$$Nu \sim Ra^{1/5} Pr^0, \quad Re \sim Ra^{3/5} Pr^{-1}. \quad (14)$$

The scaling behavior  $Nu \sim Ra^{1/5}$  has earlier been suggested by Roberts [14]. Note that in all three very large  $Pr$  regimes  $Nu$  does not depend on  $Pr$ . Furthermore the Constantin-Doering [15] upper bound  $Nu \leq \text{const} Ra^{1/3} (1 + \log Ra)^{2/3}$ , holding in the limit  $Pr \rightarrow \infty$ , is strictly fulfilled.

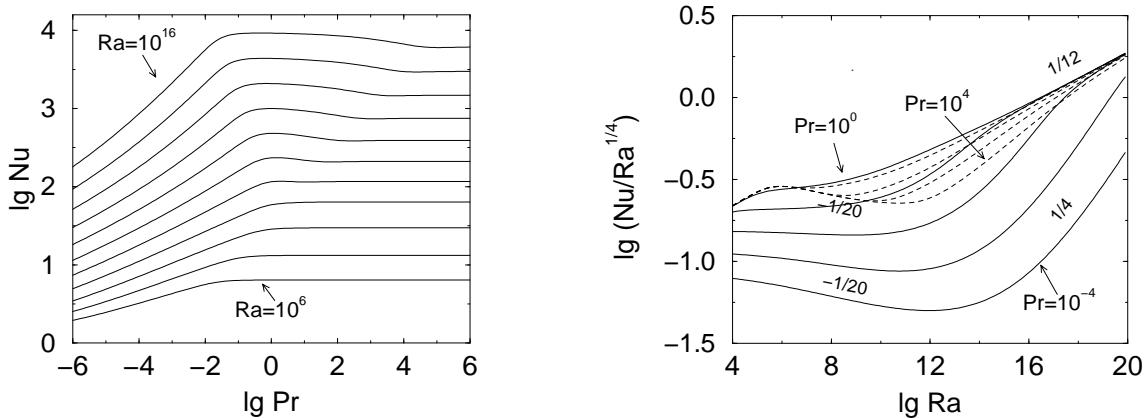


FIG. 2. (a)  $Nu$  as a function of  $Pr$  according to theory for  $Ra = 10^6, Ra = 10^7, \dots$  to  $Ra = 10^{16}$ , bottom to top. (b)  $Nu/Ra^{1/4}$  as function of  $Ra$  for  $Pr = 10^{-4}, Pr = 10^{-3}, Pr = 10^{-2}, Pr = 10^{-1}$ , and  $Pr = 10^0$  (solid lines, bottom to top) and for  $Pr = 10^1, Pr = 10^2, Pr = 10^3$ , and  $Pr = 10^4$  (dashed lines, top to bottom).

*Nu and Re in the whole parameter plane:* Plugging now the general expressions for the local dissipation rates (3), (9), (10), and (13) into the balance eqs. (1) and (2) finally results in

$$NuRaPr^{-2} = c_1 \frac{Re^2}{g(7/\sqrt{Re})} + c_2 Re^3, \quad (15)$$

$$Nu = c_3 Re^{1/2} Pr^{1/2} \left[ f \left( c_\theta \frac{Nu}{14} g \left( \frac{7}{\sqrt{Re}} \right) \right) \right]^{1/2} + c_4 Pr Re f \left( c_\theta \frac{Nu}{14} g \left( \frac{7}{\sqrt{Re}} \right) \right). \quad (16)$$

Here we have added dimensionless prefactors where appropriate to complete the modeling of the dissipation rates. In ref. [1]  $c_1$  through  $c_5$  were already adopted to Chavanne et al.'s experimental data [5]. The result was  $c_1 = 1028$ ,  $c_2 = 9.38$ ,  $c_3 = 1.42$ ,  $c_4 = 0.0123$ ,  $1/c_\theta = c_5 = 2.0$ , see eqs. (4.4) through (4.9) of [1]. Note that the  $c_i$  may depend on the aspect ratio and are not universal.

The set of eqs.(15) and (16) is the second main result of this paper. It allows to calculate  $Nu(Ra, Pr)$  and  $Re(Ra, Pr)$  in the whole  $Ra - Pr$  parameter space, including all crossovers from any regime to any neighboring one. Technically, eq. (15) is solved for  $Nu(Ra, Re, Pr)$  which then is inserted into eq. (16), leading to *one* implicit equation for  $Re(Ra, Pr)$ .

All limiting, pure scaling regimes which can be derived from eqs. (15) and (16) are listed in table I which extends table II of ref. [1], now including the three new regimes  $I_\infty^<$ ,  $I_\infty^>$ , and  $III_\infty$ . The corresponding phase diagram is shown in figure 1, completing that of [1] towards very large  $Pr$ .

Though in the phase diagram we have drawn lines to indicate transitions between the regimes, defined by either  $\epsilon_{u,BL} = \epsilon_{u,bulk}$  or  $\epsilon_{\theta,BL} = \epsilon_{\theta,bulk}$  or  $\lambda_u = \lambda_\theta$  or  $\lambda_u = L/28$ , we note that the crossovers are nothing at all but sharp. All transitions are smeared out over broad ranges, the more, the more similar the scaling exponents of the neighboring regimes are.

*Discussion of  $Nu(Pr)$  and  $Nu(Ra)$ :* The functions  $Nu(Pr)$  (for fixed values of  $Ra$ ) and  $Nu(Ra)/Ra^{1/4}$  (for fixed values of  $Pr$ ) resulting from eqs. (15) - (16) are shown in figure 2. Indeed, for  $Ra \approx 10^6 - 10^9$  the Nusselt number saturates with increasing  $Pr$  and the regime  $I_u$  with  $Nu \sim Pr^{-1/12}$  is suppressed, in full agreement with the experimental and numerical results [9–11]. However, for larger  $Ra$  beyond  $\approx 10^{11}$  the theory predicts a maximum for the curve  $Nu(Pr)$ . The decreasing branches of the curve for  $Ra \approx 10^{12}$  and  $Pr \approx 50$  may be consistent with above mentioned experimental results by Ashkenazi and Steinberg [7]. This observation may resolve the apparent discrepancy between the Ahlers et al. and the Steinberg et al. data: Simply different regimes in the  $Ra - Pr$  phase space are probed.

The importance of transition ranges is highlighted in fig. 2b. E.g., in regime  $II_l$  with  $Nu \sim Ra^{1/5}$  (for fixed  $Pr$ ) the corresponding scaling exponent  $1/5 - 1/4 = -1/20$  only becomes observable for very small  $Pr \approx 10^{-3} - 10^{-4}$ . At  $Pr = 10^{-2}$  the roughly four decades of regime  $II_l$  (see figure 1) between regime  $I_l$  and  $IV_l$ , which both have a stronger  $Ra$  dependence of  $Nu$ , are not sufficient to reveal the scaling exponent. And at  $Pr = 10^{-1}$  the roughly 2.5 decades of regime  $II_l$  are *nowhere* sufficient to lead to a local scaling exponent  $dNu/dRa$  smaller than  $1/4$ !

Similarly, for  $Pr = 1$  only for very large  $Ra \gtrsim 10^{15}$  pure scaling  $Nu \sim Ra^{1/3}$  is revealed. For smaller  $Ra$  regimes  $I_u$  and  $I_l$  with  $Nu \sim Ra^{1/4}$  strongly contribute, resulting in an

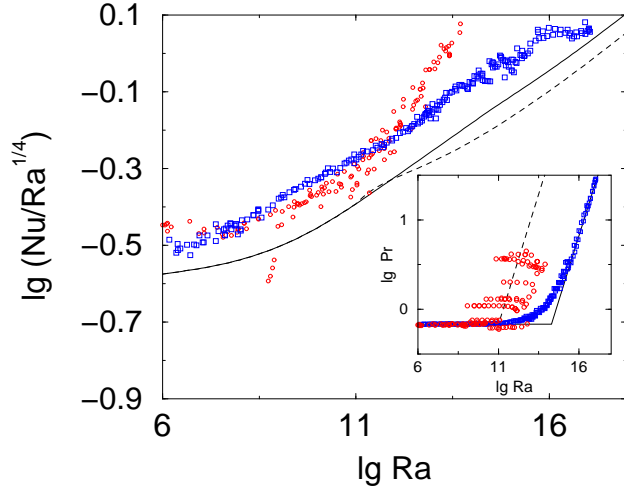


FIG. 3.  $Nu(Ra, Pr(Ra))/Ra^{1/4}$  along the curve  $Pr(Ra)$  given by the experimental restrictions of either the Niemela et al. experiment [6] (boxes in the inset and solid line in the main figure; the experimental data itself are shown as boxes) or the Chavanne et al. experiment [5] (circles in the inset and dashed line in the main figure; the experimental data itself are shown as circles). The simple parameterizations on which the curves in the main figures are based are also indicated.

effective local scaling exponent (increasing with  $Ra$ ) in the range between 0.28 (“2/7”) and 0.31, just as observed in experiment [2, 3, 5, 6].

*Direct comparison to experiment:* Finally, let us point out that the present approach simplifies the comparison with experimental data: In experiment, it is hard to vary either  $Ra$  or  $Pr$  over many decades *and* at the same time to keep the other variable fixed. So most measurements are done along *curved* lines in the phase space figure 1, mixing the  $Ra$  and  $Pr$  dependences. Now eqs. (15) and (16) allow to calculate  $Nu$  and  $Re$  along such a curve  $Pr(Ra)$  given by the experimental restrictions, which connect  $Ra$  and  $Pr$ . E.g., figure 3 shows  $Nu(Ra, Pr(Ra))$  with  $Pr(Ra)$  as resulting from the Niemela et al. [6] and the Chavanne et al. [5] experiments.

The present theory suggests that beyond  $Ra \approx 10^{12}$  the Nusselt number in the Chavanne et al. experiment [5] should be *smaller* than in the Niemela et al. experiment [6], in contrast to what is found. This result is also in contrast to our former speculation of ref. [1], that the strong  $Nu \sim Ra^{3/7}$  dependence of regime  $III_u$ , to which the Chavanne et al. data are closer, would account for their experimental findings. What we had overseen is that the larger  $Pr$  numbers of the Chavanne et al. experiment (for fixed  $Ra$ ) and the  $Nu \sim Pr^{-1/7}$  dependence of regime  $III_u$  overcompensates the strong  $Ra$  dependence of  $Nu$  for the Chavanne et al. data close to regime  $III_u$ .

This present theory cannot resolve the paradox between the Chavanne et al. and the Niemela et al. data. Possibly, different temperature boundary conditions have been applied. Possibly, Chavanne et al. have already observed the transition from a laminar to a turbulent kinetic BL (dotted line in the phase diagram fig. 1).

**Acknowledgement:** This research work was prompted by the experiments of G. Ahlers [9]. We thank him for sharing his results with us prior to publication and for various discussions.

- 
- [1] S. Grossmann and D. Lohse, J. Fluid. Mech. **407**, 27 (2000).
  - [2] B. Castaing *et al.*, J. Fluid Mech. **204**, 1 (1989).
  - [3] E. D. Siggia, Annu. Rev. Fluid Mech. **26**, 137 (1994).
  - [4] S. Cioni, S. Ciliberto, and J. Sommeria, J. Fluid Mech. **335**, 111 (1997).
  - [5] X. Chavanne *et al.*, Phys. Rev. Lett. **79**, 3648 (1997).
  - [6] J. Niemela, L. Skrebek, K. R. Sreenivasan, and R. Donnelly, Nature **404**, 837 (2000).
  - [7] S. Ashkenazi and V. Steinberg, Phys. Rev. Lett. **83**, 3641 (1999).
  - [8] X. Xu, K. M. S. Bajaj, and G. Ahlers, Phys. Rev. Lett. **84**, 4357 (2000).
  - [9] G. Ahlers, 2000, seminar at the ITP-Workshop in Santa Barabara.
  - [10] R. Verzicco and R. Camussi, J. Fluid Mech. **383**, 55 (1999).
  - [11] J. Herring and R. Kerr, Preprint (2000).
  - [12] L. D. Landau and E. M. Lifshitz, *Fluid Mechanics* (Pergamon Press, Oxford, 1987).
  - [13] B. I. Shraiman and E. D. Siggia, Phys. Rev. A **42**, 3650 (1990).
  - [14] G. O. Roberts, Geophys. Astrophys. Fluid Dyn. **12**, 235 (1979).
  - [15] P. Constantin and C. Doering, J. Stat. Phys. **94**, 159 (1999).